IMPULSIVE NOISE OF PARTIAL DISCHARGE AND ITS IMPACT ON MINIMUM DISTANCE-BASED PRECODER OF MIMO SYSTEM

Ghadir Madi[1], *Baptiste Vrigneau*[1], *Yannis Pousset*[1], *Rodolphe Vauzelle*[1], *and Basile L. Agba*[2]

[1] Poitiers University, XLIM-SIC Laboratory CNRS UMR 6172
Téléport 2, Bd Marie et Pierre Curie, BP 30179 86962 Futuroscope Cedex (France)
[2] Hydro-Québec's Research Institute, 1800 Lionel-Boulet, Varennes (Québec) Canada
phone: + (33) 549496592, fax: + (33) 549496570
email: madi, vrigneau, pousset, vauzelle@sic.univ-poitiers.fr, agba.basile@ireq.ca
web:www.sic.sp2mi.univ-poitiers.fr

ABSTRACT

Impulsive interference has been measured recently in some wireless communication environments. By using measured data of partial discharge, we show in this paper that the Middleton Class A model can approximate the impulsive noise in an electricity substation better than the Gaussian noise. The measured data was obtained from Hydro-Québec's Research Institute in cooperation with ETS (École de technologie supérieure of Montreal). We derive an extension of Middleton Class A model for multi-antenna systems. Using this model with estimated parameters from measured data, we evaluate the performance of two linear MIMO precoders with two spectral efficiencies (4 bit/s/Hz and 8 bit/s/Hz). The max-$d_{\min}$ *precoder optimizes the minimum Euclidean distance of the received constellation and the max-SNR or single beamforming maximizes the received SNR.*

1. INTRODUCTION

Wireless communications systems may experience several kinds of noise. In most of cases, e.g. thermal noise, it can be represented by a Gaussian model. However, wireless communications systems are seldom interfered by white Gaussian noise alone. The human-made electromagnetic (EM) environment, and much of the natural one, is basically impulsive and it can not be assumed to be Gaussian. The impulsive noise has a highly structured form characterized by significant probabilities of large interference levels and short duration [1]. The impulsive noise or electromagnetic interference (EMI) can be found in many indoor and outdoor environments [2]. The electricity substation and electrical transmission networks are a typical example of such impulsive environment, where the partial discharge (PD) and the corona effect are major sources of impulsive noise. Deployment of wireless communications (sensor network for example) in electricity substation for monitoring and control applications offers significant benefits over wired communications [3, 4]. Since wireless networks do not use expensive signal and control cables for data transmission, they are easier to install and use, and provide a cost-effective solutions for these applications. However, the impulsive character of the interference can drastically degrade the performance and the reliability of wireless communications systems even in case of high signal to noise ratios (SNR). In order to guard against unacceptable performance, the true characteristics of the noise must be taken into account. To do so, one needs an accurate model for the impulsive noise.

Statistical-physical models of EMI have been derived by Middleton with three models (class A, B and C) including the non-Gaussian components of natural and human-made noise [5]. The models are parametric with parameters explicitly determined by the underlying physical mechanisms, and are canonical i.e. their mathematical form is independent of the physical environment. The distinction between the three models is based on the relative bandwidth of noise and receiver. Middleton models have been shown to accurately model the non-linear phenomenon governing electromagnetic interference. These models have been widely used in electromagnetic applications and communication problems [1, 6, 7]. In [7], for example, it was demonstrated that radio frequency interference (RFI) in a computation platform (e.g. laptop computer) is well modeled using the Middleton Class A model. In this paper, our goal is to validate this statistical model for an electricity substation by using measured data and show its impact in (2×2), (2×4) and (4×4) MIMO systems.

This paper is organized as follows: section 2 introduces a brief overview of the Middleton Class A model. Section 3 focuses on the validation of the Middleton Class A model with measured data of partial discharge. The MIMO system based on max-$d_{\min}$ solution and the extension of Middleton Class A model for multi-antenna systems are presented in section 4. Performances in terms of bit error rate (BER) are presented in section 5.

2. MIDDLETON CLASS A MODEL

Middleton Class A model refers to Narrowband Noise where interference spectrum is narrower than the receiver bandwidth. In this model, the received interference is assumed to be a process having two components [1, 5]:

$$X(t) = X_P(t) + X_G(t) \tag{1}$$

where $X_P(t)$ and $X_G(t)$ are independent processes. They represent the non-Gaussian (impulsive) and Gaussian components respectively. The probability density function (PDF) of $X(t)$ is given in [1]:

$$f_{P+G}(x) = e^{-A}\sum_{m=0}^{\infty}\frac{A^m}{m!\sqrt{2\pi\sigma_m^2}}\; e^{\frac{-x^2}{2\sigma_m^2}} \text{ with } \sigma_m^2 = \frac{\frac{m}{A}+\Gamma}{1+\Gamma} \tag{2}$$

Note that f is a weighted sum of zero-mean Gaussians with increasing variance. A and Γ are the basic parameters of the model. Let us consider their definitions and physical significance:

1) A is the Overlap Index or Nonstructure Index.

$$A = \nu T_s \tag{3}$$

where ν is the average number of emission events impinging on the receiver per second and T_s is the mean duration of a typical interfering source emission. The smaller A is, the fewer the number of emission (events) and/or their durations. Therefore, the (instantaneous) noise properties are dominated by the waveform characteristics of individual events. As A is made larger, the noise becomes less structured, i.e., the statistics of the instantaneous amplitude approach the Gaussian distribution (according to central limit theory [5]). Hence, A is a measure of the non-Gaussian nature of the noise input to the receiver.
2) Γ is called the Gaussian factor. It is the ratio of powers in the Gaussian and non-Gaussian components

$$\Gamma = \frac{\langle X_G \rangle}{\langle X_P \rangle} \tag{4}$$

In general, $A \in [10^{-4}, 1]$ and $\Gamma \in [10^{-6}, 1]$ [8]. By adjusting the parameters A and Γ, the density in (2) can be made to fit a great variety of non-Gaussian noise densities.

3. VALIDATION OF MIDDLETON CLASS A MODEL FOR PARTIAL DISCHARGE

This work has been done in scientific collaboration between XLIM-SIC laboratory, Hydro-Québec's Research Institute and ETS as part of project for wireless sensor communication in disturbed environments. The electricity substation is an example of such environment where the partial discharge (PD) is a major source of impulsive noise. The PD is a result of incomplete electrical breakdown in insulating dielectrics resulting in an impulsive and component of current. Hence, three specimens have been used in a laboratory of ETS in order to reproduce the PD and measure the impulsive noise. Therefore, they have provided us with three measured datasets. We validated the Middleton Class A model with the measured noise by the following procedure of Figure 1. From the measured noise, we used the method of moments [9] to estimate the parameters A and Γ of Middleton Class A model:

$$A_{est} = \frac{9(e_4 - 2e_2^2)^3}{2(e_6 + 12e_2^3 - 9e_2e_4)^2} \tag{5}$$

$$\Gamma_{est} = \frac{2e_2(e_6 + 12e_2^3 - 9e_2e_4)}{3(e_4 - 2e_2^2)^3} \tag{6}$$

where e_2, e_4 and e_6 are the second, the fourth and the sixth order moments of the envelope data respectively. These estimated parameters will then be used to generate the noise.

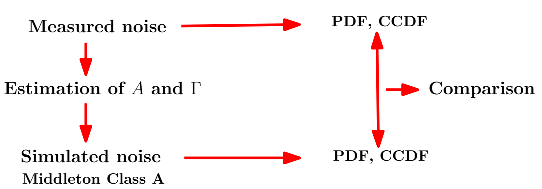

Figure 1: Procedure of validation of Middleton Class A model

In the procedure for validation, three statistical methods are used to compare measured and simulated noises:
1) The probability density function (PDF) is estimated from measured data by using kernel density estimators [10]. A set of 10^5 noise samples were used in estimation.
2) The complementary cumulative distribution function (CCDF) gives the probability that the random variable is above a particular level and is defined as:

$$\mathrm{CCDF}(x) = P(x > a) = \int_x^{\infty} \mathrm{PDF}(x)dx = 1 - \mathrm{CDF}(x) \tag{7}$$

where CDF is the cumulative distribution function.
3) The Kullback-Leibler divergence (K-L) measures the dissimilarity between two probability distributions P and Q, where (K-L)= 0 indicates that $P = Q$ [11].
Figures 2 and 3 show both PDF and CCDF for two measured noises. Table 1 presents The K-L divergences of measured noise and the two models of noise. These results show that the measured impulsive noise is better modeled by the Middleton Class A model as compared to Gaussian noise. Hence, we can use the Middleton Class A as an approximated model for impulsive noise in electricity substation. Therefore, we evaluate the performance of wireless communication in such environment by using the estimated parameters.

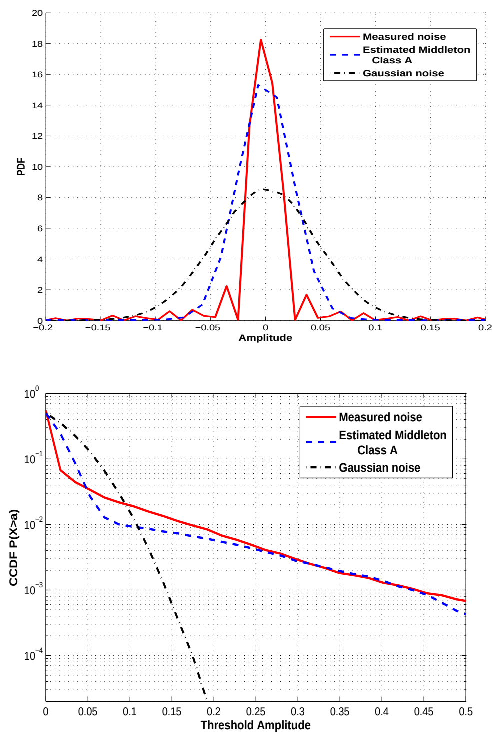

Figure 2: Measured Noise-1 PDF and CCDF, estimated parameters: $A_{est} = 0.0280$, $\Gamma_{est} = 0.3978$

	Measured noise-1	Measured noise-2
Class A	0.04	0.02
Gaussian	0.3	0.27

Table 1: K-L divergences

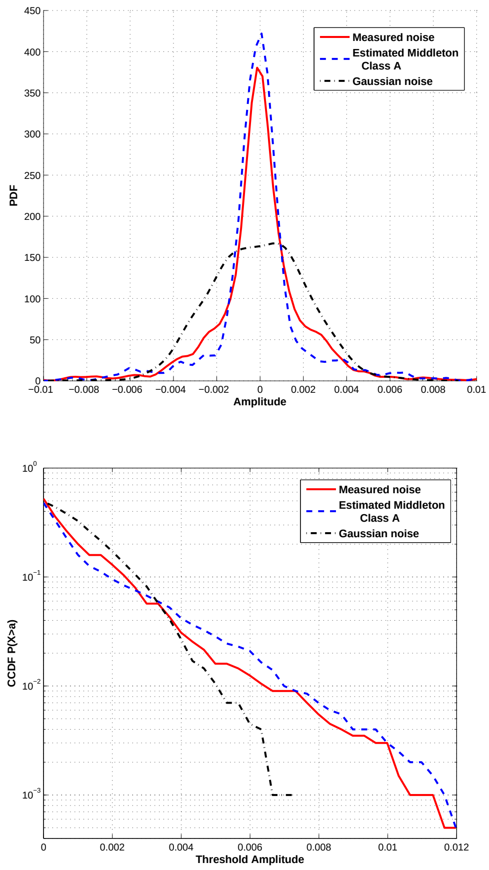

Figure 3: Measured Noise-2 PDF and CCDF, estimated parameters: $A_{est} = 0.3575$, $\Gamma_{est} = 0.1194$

4. MIMO SYSTEM AND NOISE MODEL FOR MULTI-ANTENNA SYSTEMS

Our research focuses on the wireless sensor communication in disturbed environments. Recently, there has been a great amount of research on various MIMO techniques for wireless communication systems, more particularly cooperative MIMO and virtual antenna array concepts have been proposed to achieve MIMO capability in sensor networks [12]. In [12] the results showed that in some cases, cooperative MIMO based sensor networks may lead to better energy optimization and smaller end-to-end delay. Therefore, we consider a MIMO system to evaluate the impact of the impulsive noise. The MIMO system is based on a linear precoder with the assumption that the channel state information (CSI) is available at both transmit and receive side. The use of CSI allows designing linear precoders by optimizing a pertinent criteria such as maximizing the received Signal-to-Noise Ratio (max-SNR or beamforming), minimizing the mean square error (MMSE), maximizing the capacity (Water-Filling solution) [13] or the maximization of the minimum Euclidean distance of received constellation (max-$d_{\min}$ solution) [14]. The max-$d_{\min}$ precoder achieves good performances in terms of BER providing a significant gain of SNR compared to other precoders [15] and it will be used in our MIMO system.

4.1 Linear precoder and max-$d_{\min}$ solution

Let us consider a MIMO system with n_t transmit and n_r receive antennas over which we want to achieve b independent data streams ($b \leq \min(n_t, n_r)$). The received signal can then be expressed as:

$$\mathbf{y} = \mathbf{GHFs} + \mathbf{Gv} \tag{8}$$

where $\mathbf{y}$ is the $b \times 1$ received vector, $\mathbf{s}$ is the $b \times 1$ symbols vector of the constellation C, $\mathbf{v}$ is an additive noise vector of size $n_r \times 1$, $\mathbf{H}$ is the channel matrix, $\mathbf{F}$ and $\mathbf{G}$ are the precoder and decoder matrices, respectively. In our case, the additive noise is the Middleton Class A model. The CSI permits the precoder to diagonalize the channel:

$$\mathbf{y} = \mathbf{G}_D\mathbf{H}_v\mathbf{F}_D\mathbf{s} + \mathbf{G}_D\mathbf{v}_v \tag{9}$$

where $\mathbf{H}_v = \mathbf{G}_v\mathbf{H}\mathbf{F}_v = \mathrm{diag}(\sigma_1, \ldots, \sigma_b)$ is the virtual channel matrix of size $b \times b$, σ_i stands for every subchannel gain (sorted by decreasing order), $\mathbf{v}_v = \mathbf{G}_v\mathbf{v}$ is the virtual noise, $\mathbf{F}_D$ and $\mathbf{G}_D$ are $b \times b$ matrices, representing the precoder and decoder in the virtual channel. The power constraint is expressed as $\mathrm{trace}\{\mathbf{FF}^*\} = \mathrm{trace}\{\mathbf{F}_D\mathbf{F}_D^*\} = p_o$ where p_o is the mean available transmit power. As only a maximum Likelihood (ML) detection is considered in the rest of the paper, the decoder matrix $\mathbf{G}_D$ has no impact on the performance and is consequently assumed to be $\mathbf{G}_D = \mathbf{I}_b$, with $\mathbf{I}_b$ the identity matrix of size $b \times b$. The minimum Euclidean distance between signal points at the receiver side $d_{\min}$ is defined by :

$$d_{\min}(\mathbf{F}_d) = \min_{(\mathbf{s}_k,\mathbf{s}_l)\in C^b, \mathbf{s}_k \neq \mathbf{s}_l} \|\mathbf{H}_v\mathbf{F}_d(\mathbf{s}_k - \mathbf{s}_l)\| \tag{10}$$

where $\mathbf{s}_k$ and $\mathbf{s}_l$ are 2 symbols vector whose entries are elements of C. Then, the max-$d_{\min}$ precoder is the solution of:

$$\mathbf{F}_D = \arg\max_{\mathbf{F}_d} \, d_{\min}(\mathbf{F}_d) \tag{11}$$

A very exploitable solution of (11) is given in [14] for two independent data streams, $b = 2$ and a 4-QAM with a spectral efficiency of 4 $bit/s/Hz$. Recently, the solution with two 16-QAM symbols was also given [16]. This extension permits to increase the spectral efficiency to 8 $bit/s/Hz$.

4.2 Extension of Middleton Class A model

Middleton Class A model was derived for single antenna systems. For a two-antenna system, we considered a bivariate Middleton Class A model used in [7]. This model is limited to $n_r = 2$ antennas. Thus, we derive an extension for $n_r \geq 2$. We can write (2) as

$$f(x) = \sum_{m=0}^{\infty} a_m g(x, \mu, \sigma_m^2) \tag{12}$$

where $a_m = \frac{e^{-A}A^m}{m!}$, $\mu = 0$ and $g(x, \sigma_m^2) = \frac{1}{\sqrt{2\pi\sigma_m^2}} e^{\frac{-x^2}{2\sigma_m^2}}$. The density of Middleton Class A can be approximated by the two-term model ($m = 0, 1$) [8]

$$f(x) = e^{-A}g(x, \sigma_0^2) + (1 - e^{-A})g(x, \sigma_1^2) \tag{13}$$

Let $x = [x_1, x_2, x_3, \ldots, x_k]$ be a vector of $k = n_r$ random variables, each variable has a Middleton Class A density function

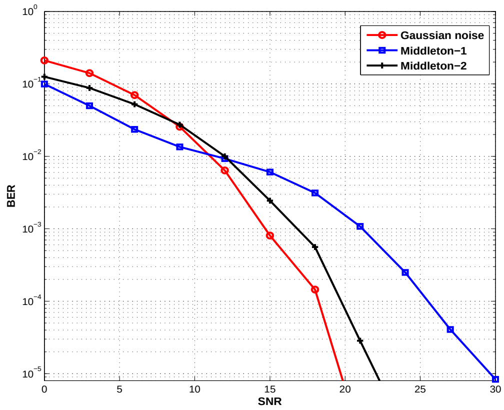

Figure 4: BER of max-$d_{\min}$ 2 symbols 4-QAM, 2×2 MIMO, ($4\ bit/s/Hz$)

and x_k is the noise observation at the k^{th} antenna. Then, the multivariate density of x can be written as [8]

$$f_x(x) = \sum_{m=0}^{\infty} a_m g(x, K_m) \tag{14}$$

where a_m is as in (12), K is the covariance matrix which represents the spatial correlation in the noise and g is a multivariate Gaussian function

$$g_x(x) = \frac{1}{(2\pi)^{\frac{n_r}{2}} |K|^{\frac{1}{2}}} e^{\frac{-x^T K^{-1} x}{2}} \tag{15}$$

where $|.|$ denotes the determinant. From (14) and (15) we obtain

$$f_x(x) = \sum_{m=0}^{\infty} \frac{a_m}{(2\pi)^{\frac{n_r}{2}} |K_m|^{\frac{1}{2}}} e^{\frac{-x^T K_m^{-1} x}{2}} \tag{16}$$

Equation (16) represents a general extension of Middleton Class A model for multi-antenna systems. We can use the approximation as in (13) for ($m = 0, 1$). Then, we obtain an approximate version of the extension

$$f_x(x) = \frac{e^{-A}}{(2\pi)^{\frac{n_r}{2}} |K_0|^{\frac{1}{2}}} e^{\frac{-x^T K_0^{-1} x}{2}} + \frac{1 - e^{-A}}{(2\pi)^{\frac{n_r}{2}} |K_1|^{\frac{1}{2}}} e^{\frac{-x^T K_1^{-1} x}{2}} \tag{17}$$

where K_m is $n_r \times n_r$ covariance matrix and is defined as

$$K_m = \begin{pmatrix} Var(x_1)_m & \dots & Cov(x_1, x_k)_m \\ \vdots & \ddots & \vdots \\ Cov(x_k, x_1)_m & \dots & Var(x_k)_m \end{pmatrix} \tag{18}$$

$$\text{where} \begin{cases} Var(x_k)_m = \frac{\frac{m}{A} + \Gamma_k}{1 + \Gamma_k} = \sigma_{km}^2 \\ \\ Cov(x_i, x_j)_m = \rho_{ij} \sigma_{im} \sigma_{jm} \end{cases}.$$

Γ_k is the Gaussian factor at the k^{th} antenna and ρ_{ij} is the correlation coefficient between the noise observations at i and j antennas, $-1 \le \rho \le 1$. Finally, we can write K_m as

$$K_m = \begin{pmatrix} \sigma_{1m}^2 & \dots & \rho_{1k} \sigma_{1m} \sigma_{km} \\ \vdots & \ddots & \vdots \\ \rho_{k1} \sigma_{km} \sigma_{1m} & \dots & \sigma_{km}^2 \end{pmatrix} \tag{19}$$

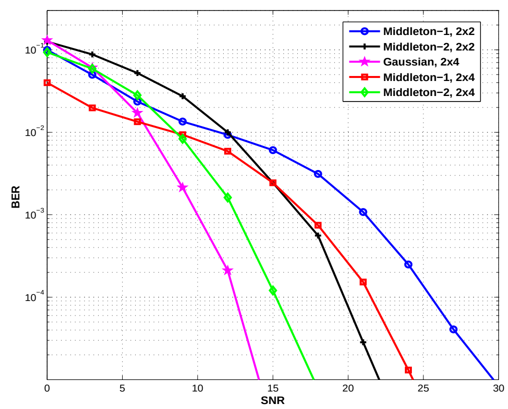

Figure 5: BER of max-$d_{\min}$ 2 symbols 4-QAM, 2×2 and 2×4 MIMO, ($4\ bit/s/Hz$), (Middleton-1: $A_{est} = 0.0280$, $\Gamma_{est} = 0.3978$), (Middleton-2: $A_{est} = 0.3575$, $\Gamma_{est} = 0.1194$)

5. SIMULATION RESULTS

The performance of MIMO precoders presented in section 4 are evaluated in terms of BER in presence of impulsive noise. The parameters A and Γ estimated in section 3 were used to generate the corresponding noise. For the noise model in multi-antenna system, we considered a simple case ($\Gamma_{est} = \Gamma_1 = \Gamma_2 = \ldots = \Gamma_{n_r}$ and $\rho_{ij} = \rho_{ji} = 0$) to calculate the covariance matrix. The max-$d_{\min}$ precoder uses two symbols with QAM modulation, and an ML detection. The Middleton Class A model is defined for only real sample observation. For complex signals (QAM modulation), we assume that the real and the imaginary parts of the signal are independent and identically distributed (*i.i.d*). We considered a traditional ML receiver, i.e., an ML receiver designed for Gaussian distributed noise. A flat Rayleigh-fading channel was used, i.e., $\mathbf{H}$ is an ($n_r \times n_t$) channel matrix with independent and identical distributed complex Gaussian entries with mean zero and unit variance. We simulated the max-$d_{\min}$ precoder in several cases: with 4-QAM or 16-QAM, (2×2), (2×4) or (4×4) MIMO systems.

Figure 4 shows a degradation of BER of the max-$d_{\min}$ precoder (2×2 MIMO) in the presence of impulsive noise. The energy of the Middleton Class A model is a sum of two components of noise (Gaussian and impulsive). At low SNR, the BER is sensitive to the Gaussian component of the Middleton Class A noise, which has lower energy than a classical Gaussian noise. Hence, BER of Middleton Class A is better compared to classical Gaussian noise at low SNR. At high SNR, the MIMO system becomes sensitive to the impulsive component and this degrades the performance of the wireless systems in EMI (SNR loss can reach 5dB). *Middleton-1* and *Middleton-2* denote the estimated noises for ($A_{est} = 0.0280$, $\Gamma_{est} = 0.3978$) and ($A_{est} = 0.3575$, $\Gamma_{est} = 0.1194$) respectively. When the value of A_{est} increases, the Gaussian component increases and the BER of *Middleton-2* is close to the Gaussian case. Moreover, Figure 5 shows the influence of the number of receive antennas. When we increased n_r from 2 to 4, the BER is improved with a SNR gain near 4 dB. We can also observe that the impulsive noise influence the diversity order. Indeed, the max-$d_{\min}$ precoder achieves the maximum diversity order $n_t \times n_r$ in the Gaussian case. In the Middleton case, the diversity is lower.

For 2×2 MIMO system and a perfect or imperfect CSI,

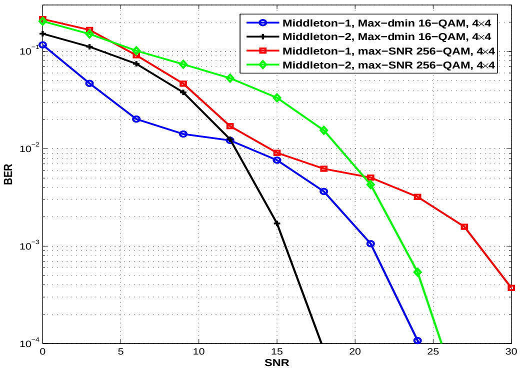

Figure 6: BER of max-$d_{\min}$ 2 symbols 16-QAM and max-SNR one symbol 256-QAM, 4×4 MIMO, (8 $bit/s/Hz$), (Middleton-1: $A_{est} = 0.0280$, $\Gamma_{est} = 0.3978$), (Middleton-2: $A_{est} = 0.3575$, $\Gamma_{est} = 0.1194$)

we showed in [17] that the max-$d_{\min}$ 16-QAM precoder achieved a better BER than the max-SNR (256-QAM) one with a spectral efficiency of 8 $bit/s/Hz$ and a Gaussian noise. This performance of max-$d_{\min}$ 16-QAM is also similar for 4×4 MIMO and Gaussian noise. Hence, we evaluated the performance of these precoders with 4×4 MIMO system and the impulsive noise model in Subsection 4.2 . Figure 6 shows that the max-$d_{\min}$ 16-QAM is still the best. However, in the case of *Middleton-1*, i.e. with an impulsive component, behaviors of precoders are different. The max-$d_{\min}$ has a significant SNR gain on the max-SNR except when the SNR is about 15 dB. The two precoders are then close. It means that the max-$d_{\min}$ is more sensitive to the transition of the impulsive noise with a particular SNR.

6. CONCLUSION

In this paper, we used a Middleton Class A model in order to model the noise of an electricity substation. We validated this model with measured data of different sort of partial discharge and the estimated paramaters can be used to evaluate BER of MIMO systems. A simple extension of the model was derived for multi-antenna systems in order to evaluate the performance of linear precoders for MIMO systems in presence of impulsive noise. The results showed that with a high SNR (which is desirable in communication systems), the performance of the linear precoder was degraded in the presence of impulse noise compared to a Gaussian case. Future research tracks might concern the following: 1) the optimization of the max-$d_{\min}$ precoder for the impulsive noise model and 2) the validation of the multi-antenna extension with measured data.

Acknowledgments

This work was supported by the Franco-Québec Champlain program and the french ANR MOCAMIMODYN project.

REFERENCES

[1] A. Spaulding and D. Middleton, "Optimum reception in an impulsive interference environment-part 1: Coherent detection," *IEEE Transactions on Communications*, no. 9, pp. 910–923, sept. 1977.

[2] J. D. Parsons, *The Mobile Radio Propagation Channel*. New York: Wiley, 1996.

[3] A. Willig, K. Matheus, and A. Wolisz, "Wireless technology in industrial networks," *Proceedings of the IEEE*, vol. 93, pp. 1130–1151, 2005.

[4] A. Shapoury and M. Kezunovic, "Noise profile of wireless channels in high voltage substations," *IEEE Power Engineering Society General Meeting*, 2007.

[5] D. Middleton, "Non-gaussian noise models in signal processing for telecommunications: New methods and results for class A and class B noise models," *IEEE Transactions on Information Theory*, vol. 45, no. 4, pp. 1129–1149, May 1999.

[6] S. Miyamoto, M. Katayama, and N. Morinaga, "Performance analysis of QAM systems under class A impulsive noise environment," *IEEE Transactions on Electromagnetic Compatibility*, vol. 37, no. 2, pp. 260–267, May 1995.

[7] K. Gulati, A. Chopra, R. Heath, B. Evans, K. Tinsley, and X. Lin, "MIMO receiver design in the presence of radio frequency interference," *IEEE Global Communications Conference*, 2008.

[8] P. A. Delaney, "Signal detection in multivariate class A interference," *IEEE Transactions on Communications*, vol. 43, no. 2, pp. 365–373, 1995.

[9] D. Middleton, "Procedures for determining the properties of the first-order canonical models of class A and class B electromagnetic interference," *IEEE Transactions on Electromagnetic Compatibility*, vol. 21, pp. 190–208, Aug. 1979.

[10] Z. I. Botev, "A novel nonparametric density estimator," *The University of Queensland, Tech. Rep*, Nov. 2006.

[11] S. Kullback, *Information Theory and Statistics*. Peter Smith, 1978.

[12] S. Cui, A. J. Goldsmith, and A. Bahai, "Energy-efficiency of MIMO and cooperative MIMO techniques in sensor networks," *IEEE Journal on Selected Areas in Communications*, vol. 22, no. 6, 2003.

[13] H. Sampath, P. Stoica, and A. Paulraj, "Generalized linear precoder and decoder design for MIMO channels using the weighted MMSE criterion," *IEEE Transactions on Communications*, vol. 49, no. 12, pp. 2198–2206, Dec. 2001.

[14] L. Collin, O. Berder, P. Rostaing, and G. Burel, "Optimal minimum distance-based precoder for MIMO spatial multiplexing systems," *IEEE Transactions on Signal Processing*, vol. 52, no. 3, pp. 617–627, 2004.

[15] B. Vrigneau, J. Letessier, P. Rostaing, L. Collin, and G. Burel, "Statistical comparison between max-dmin, max-SNR and MMSE precoders." *40th Asilomar Conference on Signals, Systems and Computers*, Oct. 2006.

[16] Quoc-tuong, O. Berder, B. Vrigneau, and O. Sentieys, "Minimum distance based precoder for MIMO-OFDM systems using a 16-QAM modulation," *IEEE International Conference on Communications, Germany*, 2009.

[17] G. Madi, B. Vrigneau, Y. Pousset, and R. Vauzelle, "A realistic MIMO time-variant channel applied to diagonalizing precoders," *The 9th International Conference on ITS Telecommunications, France*, Oct. 2009.